Revisiting substrate-induced bianisotropy in metasurfaces

M. Albooyeh,[1] R. Alaee,[2] C. Rockstuhl,[2,3] and C. Simovski[1,4]

[1]*Department of Radio Science and Engineering/SMARAD Centre of Excellence, Aalto University, P.O. Box 13000, FI-00076 Aalto, Finland*

[2]*Institute of Theoretical Solid State Physics, Karlsruhe Institute of Technology, 76131 Karlsruhe, Germany*

[3]*Institute of Nanotechnology, Karlsruhe Institute of Technology, 76021 Karlsruhe, Germany*

[4]*Laboratory of Metamaterials, University for Information Technology, Mechanics and Optics (ITMO), St. Petersburg 197101, Russia*

(Received 19 November 2014; revised manuscript received 5 April 2015; published 7 May 2015)

Recently, it has been shown that a metasurface of plasmonic nanospheres deposited on a highly refractive substrate requires a *bianisotropic* magnetoelectric coupling for its effective description. The effect has been coined *substrate-induced* bianisotropy. It leads to an asymmetric reflectance similar to bianisotropic metasurfaces. In this work, through a circuit model, we show that such bianisotropy does not necessarily emerge for all substrated metasurfaces. Indeed, we show that the thickness of the metasurface plays a crucial role to encounter substrate-induced bianisotropy. Moreover, by taking advantage of substrate-induced bianisotropy, we present the necessary conditions for the circuit model parameters to compensate the asymmetric reflectance generated by an *intrinsically* bianisotropic metasurface. We finally express that, in substrated metasurfaces, the asymmetric reflectance and the bianisotropic response are two separate issues albeit with interdependencies.

DOI: 10.1103/PhysRevB.91.195304 PACS number(s): 81.05.Xj, 75.30.Kz, 78.20.Bh, 78.67.Bf

I. INTRODUCTION

Metasurfaces, optically thin sheets of metamaterials, have attracted much interest due to their versatility [1–8] and because they can be fabricated easier than bulk metamaterials. Compared to their bulk counterparts, they enable more extensive scientific exploration and promise an easier integration into applications [9]. Usually, a metasurface is an optically dense planar array of resonant inclusions. At optical frequencies, these inclusions can be simple-shaped silver or gold nanoparticles. Their properties are dominated by localized surface plasmon polaritons, which cause a resonant optical response at tunable frequencies. A metasurface representing a periodic array of gold nanopatches is shown in Fig. 1. The optical response of such a metasurface to an incident plane wave in a uniform host medium (characterized by $\eta_+ = \eta_-$, where $\eta_\pm$ is the characteristic impedance of the substrate and superstrate, respectively) and in the case of optically small nanoparticles can be safely described by that of an electric dipole. The polarizability of each particle is driven into resonance at the particle plasmon wavelength. This causes dispersion in the effective electric polarizability if the metasurface is considered at the level of homogeneous media. However, the nanoparticles cannot exist in free space but necessarily have to be deposited on a substrate.

The array can be covered with a material that closely resembles the optical properties of the substrate. But except for the situation where the substrate and superstrate are of the same material, the optical contrast between the surrounding media modifies the effective properties of the metasurface compared to the metasurface located in a uniform host medium. In Ref. [10], it is shown that a metasurface deposited on a substrate requires the consideration of bianisotropy in its effective description, leading to the term substrate-induced bianisotropy (SIB). The bianisotropy means that a magnetic polarization in the metasurface is caused by the electric field and vice versa. Moreover, SIB implies that the presence of the substrate modifies the metasurface properties. Therefore, aside from the possible electric and magnetic couplings in the metasurface, a new magnetoelectric coupling is required in its effective description [3,4,11].

Chronologically, the SIB term was first introduced by Powell *et al.* for layers of a so-called fishnet metamaterial located on a dielectric substrate. The bianisotropy was accounted for by introducing an additional omega-type (ξ) material parameter in the effective material parameters [12]. Complementary to that work, in Ref. [10], it has been described how to characterize a plasmonic metasurface deposited on top of a substrate by applying Maxwell's boundary conditions for a discontinuity between two different media.

The SIB discussed in Ref. [10] has been caused by a metasurface consisting of a substrated array of plasmonic nanoparticles. In the plasmon resonance, the array of nanoparticles may be considered as resonant electric dipoles [13]. However, the presence of the substrate induces notable mirror dipoles in the substrate [14]. If the real parts of the complex permittivities of the nanoparticle and the substrate were of the same sign, the original and mirror dipole moments would be in phase and would result only in an electric dipole moment. However, in the case of metallic nanoparticles and dielectric substrates, the permittivities of the involved materials in a specific frequency region usually have opposite signs with comparable amplitudes. This results in opposite directions of the original and mirror dipole moments which causes an additional magnetic moment. This induced magnetic moment is equivalent to the response of an effective omega particle [15]. The SIB in such situation (metasurface made from metallic nanoparticles on top of a substrate) was studied in Ref. [14] in more detail. The SIB was therefore modeled similarly to an omega particle by an effective surface susceptibility that expresses the electromagnetic coupling. Eventually, this susceptibility together with the corresponding electric and magnetic susceptibilities could effectively describe the response of the substrated metasurface to plane waves. Indeed, they allowed the correct prediction of the reflection and transmission properties of the substrated metasurface for different incidence angles [14]. The interference of the local

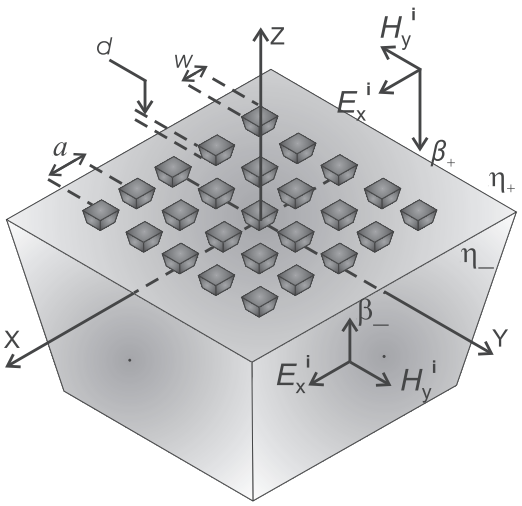

FIG. 1. A laterally (xy plane) infinite optically dense electrically resonant planar array of inclusions (gold nanopatches) at the interface ($z = 0$) of two different media with characteristic impedances η_+ for $z > 0$ and η_- for $z < 0$, respectively.

electromagnetic fields caused by the dipole and the mirror dipole are also important. A field localization and enhancement occurs around the nanoparticle. This field localization is called a hot spot here. The total field around the nanoparticle will be asymmetric with respect to the center of the nanoparticle due to the interference between the fields of the dipole and the mirror dipole. Eventually, the center of gravity of the field localization does not coincide with the center of the sphere. Instead, it is slightly displaced towards the substrate, i.e., it is asymmetric. Indeed, more index contrast between the substrate and superstrate causes larger asymmetry.

Based on the studies in Refs. [10,12], it might be naturally presumed that all substrated metasurfaces require for their effective description the bianisotropy term. This effect itself has been stimulating quite some research efforts as reflected by a series of publications [16–20]. However, while studying the properties of substrated layers of nanostructured graphene, we found first indications that a substrated metasurface might not always require a bianisotropic term for its effective description. Our curiosity got raised since we have been observing an asymmetric reflectance [21] for such substrated layers of nanostructured graphene, a property very common for an omega-type bianisotropic array [22,23]. Therefore, we found it timely to revisit the SIB effect in more detail and to clarify the necessity to consider a bianisotropic term in the effective description of a substrated metasurface. Understanding and answering the following questions might help to dissolve the ambiguities concerning the SIB:

1. Does a plasmonic array located on top of a highly refractive substrate always possess a considerable bianisotropy?

2. Does an asymmetric reflectance always require the bianisotropic response of a metasurface?

3. Is it possible for a bianisotropic array to have symmetric reflectance?

4. What are the conditions to observe bianisotropy for a metasurface of simple-shape plasmonic nanoparticles deposited on a substrate?

In this paper, we try to answer these questions. The first two questions are answered negatively. The bianisotropy may be negligible for some plasmonic arrays even if they are located on top of a high-permittivity semiconductor substrate. The asymmetric reflectance can be observed even for nonbianisotropic metasurfaces. The third question is answered positively: the bianisotropy may be observed together with the symmetric reflectance. Indeed, for metasurfaces in an asymmetric optical environment, the asymmetry of reflectance and the bianisotropy are two separate issues.

In order to answer the last question, we consider nanopatches in contrast to our previous works [10,14,24] with spherical particles. This allows us to study more conveniently the SIB depending on the thickness of the metasurface and to quantify its emergence with respect to the skin depth. In this case, the necessary condition to observe SIB is linked to the thickness of the patch that should exceed the skin depth of the metal. In substrated nanopatches, the aforementioned plasmonic hot spot appears at the bottom of the nanopatch. If the nanopatches are thinner than the skin depth, there is no need to introduce the SIB: the hot spot is symmetric with respect to the center of the nanopatch. No notable mirror dipole is induced and no magnetic mode is excited by the incident wave. In such situation we do not need to consider a bianisotropic response to effectively describe the substrated metasurface. The last assertion refers not only to metal plasmonic metasurfaces. We have also studied metasurfaces of graphene nanopatches operating at THz waves.

We believe that our work is important for further studies of resonant metasurfaces. First, it elucidates the link between the bianisotropy of the metasurface and the reflectance asymmetry. Second, it helps to avoid an unnecessary complexity of the homogenization model for thin metasurfaces. Third, it introduces the effect of SIB for substantially thick plasmonic particles.

II. CIRCUIT MODELING FOR METASURFACE CHARACTERIZATION

A. Problem scheme

Let us consider a dense planar periodic array of optically small resonant particles located on top of an isotropic dielectric substrate that is sufficiently highly refractive. For generality, at the moment, we assume that the particles have both electric and magnetic dipole resonances. Moreover, we consider the metasurface to be stretched in the xy plane. Furthermore, our proposed metasurface is isotropic in the xy plane (an example of such a metasurface is depicted in Fig. 1). Please note that the optically dense fishnet topology studied in Ref. [12] and its complementary cermet topology studied in Ref. [25] are special cases of such a uniaxial metasurface. The sample is illuminated at normal incidence by a plane wave as shown in Fig. 1. The plane wave can propagate either in the forward ($-z$) or in backward ($+z$) direction. The incident wave is characterized by an electric field $\mathbf{E}_{\pm}^{\mathrm{i}} = E_{\mathrm{x}}^{\mathrm{i}} \exp(\mp i\beta_{\pm} z) \exp(-i\omega t)\hat{\mathbf{x}}$, where $E_{\mathrm{x}}^{\mathrm{i}}$, $\beta_{\pm}$, ω, and $\hat{\mathbf{x}}$ denote the amplitude, propagation constant ("+" in superstrate and "−" in substrate media), angular frequency, and the x-axis unit vector, respectively. The plus/minus sign, which appears before "i" in the argument of

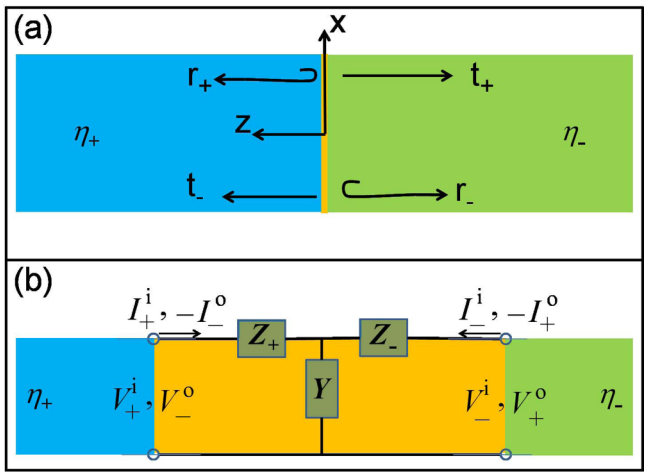

FIG. 2. (Color online) (a) Homogenous sheet model (sheet with zero thickness) of the resonant array of Fig. 1 located between two different media. (b) Circuit model for the proposed electrically resonant array at the interface of two different media.

exponential function refers to backward/forward propagation and the axis x is along the wave polarization. The propagation constant for superstrate/substrate medium is $\beta_\pm = \omega\sqrt{\mu\epsilon_\pm}$ while its characteristic impedance is $\eta_\pm = \sqrt{\mu/\epsilon_\pm}$, where μ and $\epsilon_\pm$ are the permeability and permittivity of the media, respectively. Taking into account possible magnetic properties of superstrate and substrate materials is easy, however, for the optical range $\mu = \mu_0$ and only permittivities $\epsilon_\pm$ can be different.

By illuminating the sample at normal incidence, an electric surface polarization density P_x and magnetic one M_y will be induced in the array. An ordinary homogenization model is used where the array is effectively replaced by a continuous sheet with polarization currents, as illustrated in Fig. 2(a). Now, the question is as follows: How to describe the electric P_x and the magnetic response M_y to the incident wave field? Usually, a description in terms of the so-called surface susceptibilities [25] or the circuit parameters [26] is adopted. Unlike the previously used method where the metasurface has been replaced with its effective description by a finite-thickness bulk layer, these approaches allow us to correctly predict the reflection and transmission coefficients for different angles of incidence using the same set of material parameters (electric and magnetic surface susceptibilities in Ref. [25] or impedances and admittances in Ref. [26]).

B. General comments on our circuit modeling

Prior to providing any detail, we stress that in this paper we characterize the metasurface with an equivalent circuit model approach as introduced in Ref. [26]. However, while the approach in Ref. [26] was applicable only for one illumination direction, the approach in this study is more general and applicable for both illumination directions. In the circuit model, which we will use from now on for our description, one deals with the incident, transmitted, and reflected waves in terms of effective voltages and currents. The effective properties of the metasurfaces are expressed by effective impedances. The effective impedances are related to the voltages through the currents. This allows us to use the same circuit parameters to describe the current and voltage jumps across the metasurface for both illumination directions. In an appendix, we present the link between the set of surface susceptibilities in the constitutive relations and our proposed circuit parameters. Indeed, both approaches are equivalent; the circuit parameters' notion is more common among electrical engineers while the surface susceptibilities' concept is more popular for physicists.

Generally, the impedance matrix of the metasurface can be presented by the nonsymmetric *T-circuit* scheme depicted in Fig. 2(b). Here, voltages and currents correspond to the tangential electric and magnetic fields (averaged over the metasurface unit-cell area), respectively. Equivalently, it can be replaced by a Π *circuit*. The shunt admittance Y represents the electric response while the series impedances Z_+ and Z_- correspond to the magnetic response. In addition to these points, there are some important issues related to our equivalent circuit modeling, which we mention in the following.

First, in a uniform host medium and for a metasurface with both electric and magnetic resonant couplings and without bianisotropic coupling [27], the circuit scheme is symmetric, i.e., $Z_+ = Z_-$. In the bianisotropic case, independent of whether the bianisotropy is substrate induced or intrinsic, we have $Z_+ \neq Z_-$.

Second, the expression $Z_+ = Z_- \neq 0$ can be satisfied in two different situations. On the one hand, it may correspond to the symmetric case when $\eta_+ = \eta_-$ where the metasurface has a magnetic response without bianisotropy. On the other hand, it might correspond to the situation when the SIB and the intrinsic bianisotropy of the metasurface mutually compensate.

Third, it is clear that the series impedances Z_+ and Z_- describe both bianisotropy and magnetism of the metasurface since both effects cause a magnetic polarization. However, for a nonmagnetic metasurface, which is deposited on a substrate, $Z_+ \neq Z_- \neq 0$ clearly indicates the SIB. Moreover, it is impossible to obtain $Z_+ = Z_- \neq 0$ for such nonmagnetic metasurface in the presence of a substrate. In other words, the retrieved impedances for such a metasurface must be different if they are nonzero.

C. Reflection/transmission and equivalent circuit parameters

In order to solve for the reflection $r_\pm = E_x^{\mathrm{r}}/E_x^{\mathrm{i}}$ and transmission $t_\pm = E_x^{\mathrm{t}}/E_x^{\mathrm{i}}$ coefficients of the proposed metasurface for forward/backward illumination, we use standard relations between the input and output effective voltages ($V_\pm^{\mathrm{i}}$, $V_\pm^{\mathrm{o}}$) and currents ($I_\pm^{\mathrm{i}}$, $I_\pm^{\mathrm{o}}$), respectively [28]:

$$V_\pm^{\mathrm{i}} = E_\pm^0(1 + r_\pm), \qquad I_\pm^{\mathrm{i}} = \frac{E_\pm^0}{\eta_\pm}(1 - r_\pm),$$
$$V_\pm^{\mathrm{o}} = E_\pm^0 t_\pm, \qquad I_\pm^{\mathrm{o}} = \frac{E_\pm^0}{\eta_\mp} t_\pm. \tag{1}$$

Here, $E_\pm^0$ is the effective voltage amplitude for forward/backward illumination at the input of the T circuit (E_+^0 and E_-^0 can assumed to be different). Next, the transmission matrix $[T]_\pm$, which relates the input and output voltages and currents for the T *circuit* corresponding to forward/backward

illumination direction shown in Fig. 2, reads as

$$\begin{bmatrix} V_{\pm}^{\mathrm{i}} \\ I_{\pm}^{\mathrm{i}} \end{bmatrix} = \begin{bmatrix} 1+Z_{\pm}Y & Z_{\pm}+Z_{\mp}+Z_{\pm}Z_{\mp}Y \\ Y & 1+Z_{\mp}Y \end{bmatrix} \begin{bmatrix} V_{\pm}^{\mathrm{o}} \\ I_{\pm}^{\mathrm{o}} \end{bmatrix}. \quad (2)$$

Using (1) and (2), it is possible to find the corresponding reflection and transmission coefficients for both illumination directions as following:

$$r_{\pm} = \frac{\eta_{\mp}\left(1+\frac{Z_{\mp}}{\eta_{\mp}}\right) - \eta_{\pm}\left(1-\frac{Z_{\pm}}{\eta_{\pm}}\right) - \eta_{+}\eta_{-}Y\left(1-\frac{Z_{\pm}}{\eta_{\pm}}\right)\left(1+\frac{Z_{\mp}}{\eta_{\mp}}\right)}{\eta_{+}\left(1+\frac{Z_{+}}{\eta_{+}}\right) + \eta_{-}\left(1+\frac{Z_{-}}{\eta_{-}}\right) + \eta_{+}\eta_{-}Y\left(1+\frac{Z_{+}}{\eta_{+}}\right)\left(1+\frac{Z_{-}}{\eta_{-}}\right)}, \quad (3a)$$

$$t_{\pm} = \frac{2\eta_{\mp}}{\eta_{+}\left(1+\frac{Z_{+}}{\eta_{+}}\right) + \eta_{-}\left(1+\frac{Z_{-}}{\eta_{-}}\right) + \eta_{+}\eta_{-}Y\left(1+\frac{Z_{+}}{\eta_{+}}\right)\left(1+\frac{Z_{-}}{\eta_{-}}\right)}. \quad (3b)$$

Note that Eq. (3b) automatically satisfies the reciprocity condition $t_{+}/\eta_{-} = t_{-}/\eta_{+} = t$. The effective surface impedances and admittance can be inversely retrieved as

$$\frac{Z_{\pm}}{\eta_{\pm}} = \frac{1+r_{\pm}-\alpha_{\pm}t_{\pm}}{\alpha_{\pm}-\alpha_{\pm}r_{\mp}+t_{\mp}}, \quad (4a)$$

$$\eta_{\pm}Y = \frac{1-r_{\mp}-t_{\pm}}{\left(1+\frac{Z_{\pm}}{\eta_{\pm}}\right)t_{\pm}}, \quad (4b)$$

with

$$\alpha_{\pm} = \frac{1-r_{\pm}-t_{\mp}}{1-r_{\mp}-t_{\pm}}. \quad (5)$$

Notice that even though both Eq. (4b) for η_{+} and η_{-} are apparently different, they provide identical results for Y after substitution of Eq. (4a).

There are two important consequences of Eq. (3a), which answer questions 2 and 3 formulated in the "Introduction":

(1) The reflectance $|r_{\pm}|$ may be asymmetric, i.e., $|r_{+}| \neq |r_{+}|$, even in the absence of bianisotropy. In order to prove this claim, it suffices to consider Eq. (3a) for the special case when $Y \neq 0$ and $Z_{\pm} = 0$. In this case, Eq. (3a) reduces to

$$r_{\mp} = \frac{\mp A_{-} - Y}{A_{+} + Y}, \quad (6a)$$

$$A_{\pm} = \frac{1}{\eta_{+}} \pm \frac{1}{\eta_{-}}. \quad (6b)$$

Therefore, in order to have asymmetric reflectance we must satisfy the condition

$$|r_{+}| \neq |r_{+}| \Rightarrow \mathrm{Re}\{Y A_{-}^{*}\} \neq 0. \quad (7)$$

Condition (7) implies for an electrically resonant metasurface located on top of a refractive substrate that either losses inside the metasurface or losses in the substrate (if the superstrate is lossless) are sufficient to observe an asymmetric reflectance. Both loss mechanisms cause an asymmetric reflectance. If $\mathrm{Im}(\eta_{\pm}) = 0$, the condition $\{|r_{+}| \neq |r_{-}|\}$ holds when $\mathrm{Re}\{Y\} \neq 0$ and the asymmetry is proportional to the losses. A resonantly enhanced polarization usually implies resonantly enhanced losses. This eventually suggests that the reflectance asymmetry is also resonantly enhanced. However, whereas the presence of the resonance affects the strength of the effect, this effect itself occurs already for a nonzero optical contrast between the substrate and superstrate, i.e., when $A_{-} \neq 0$. Notice in the absence of the metasurface ($Y = 0$) we have $|r_{+}| = |r_{-}|$. Beyond the resonance of the metasurface, ordinary optical losses in the media from which the two half-spaces are made offer only a slight asymmetry in the reflectance. Another issue is that the phases of the reflection coefficients are always unequal for a sandwiched layer between two different media. This is evident from Eqs. (6a) and (6b). However, due to the paper's length constraints and in order not to deviate from the main stream of the study, we do not discuss this in depth but focus instead on the amplitudes of the reflection coefficients. This is also a more convenient parameter to be measured at optical frequencies.

(2) The reflectance $|r_{\pm}|$ can be symmetric even in the presence of bianisotropy, i.e., $Z_{+} \neq Z_{-} \neq 0$. The inherent reflectance asymmetry of bianisotropic arrays may be compensated by the optical contrast between two media. Again, for simplicity we obtain conditions for a special case of this compensation. This time we consider a bianisotropic metasurface with a negligible electric response, i.e., $Y \approx 0$ but $Z_{+} \neq Z_{-} \neq 0$. For this case, Eq. (3a) reduces to

$$r_{\pm} = \frac{Z_{+} + Z_{-} \pm (\eta_{-} - \eta_{+})}{Z_{+} + Z_{-} + \eta_{-} + \eta_{+}}. \quad (8)$$

Solving Eq. (8) for $|r_{+}| = |r_{-}| = |r|$ leads to the following conditions, which must be satisfied simultaneously:

$$|r_{+}| = |r_{-}| \Rightarrow \begin{cases} \frac{\mathrm{Re}\{Z_{+}+Z_{-}\}}{\mathrm{Im}\{Z_{+}+Z_{-}\}} = -\frac{\mathrm{Im}\{\eta_{+}-\eta_{-}\}}{\mathrm{Re}\{\eta_{+}-\eta_{-}\}}, \\ \frac{|\eta_{+}-\eta_{-}|}{|\eta_{+}|+|\eta_{-}|} \leqslant |r| \leqslant 1. \end{cases} \quad (9)$$

The first condition in (9) is feasible since it requires only $\mathrm{Re}\{Z_{\pm}\} > 0$. The second condition is also feasible. It means that the reflectance from the interface without metasurface is smaller than the reflectance from the metasurface located on this interface.

With the above discussions, we have made two observations: (i) an asymmetric reflectance for a substrated metasurface does not necessarily suggest its bianisotropy, and (ii) the bianisotropy of a metasurface does not prohibit a symmetric reflectance. These two observations can be summarized as follows: the bianisotropy and asymmetry of reflectance for metasurfaces located on refractive substrates are two separate effects. Indeed, they have interdependencies but they can be observed independent from each other. The asymmetry of reflectance results from the optical contrast between the substrate and superstrate in presence of the metasurface and requires some absorption in either the metasurface or one of the surrounding media. The bianisotropy of the metasurface (intrinsic or induced by the substrate) may increase, decrease, or completely cancel this asymmetry. At one frequency, the bianisotropy described by $Z_{+} \neq Z_{-} \neq 0$ may decrease the value $|\eta_{+} - \eta_{-}|/(|\eta_{+}| + |\eta_{-}|)$ and may increase it at another frequency.

In the next step, using the formulas obtained in this section, we are ready to answer the two other motivating questions 1 and 4.

III. PRACTICAL EXAMPLES

In order to answer the other two questions 1 and 4 of the Introduction, we study examples of electrically resonant substrated metasurfaces made from plasmonic nanopatches. We will show that such metasurfaces, in spite of high optical contrast between the substrate and superstrate, are not necessarily bianisotropic. If they are sufficiently thin, they can be accurately characterized through only an effective shunt admittance Y. We consider the following scenario to characterize the substrated metasurfaces.

We first model the metasurface as a shunt admittance only without magnetic or bianisotropic response ($Y \neq 0$ and $Z_{\pm} = 0$). We next retrieve this admittance from simulated reflection and transmission data for one specific illumination scenario, i.e., illumination in the forward direction (r_+, t_+). These optical coefficients were obtained from full wave simulations of the actual structure using the Fourier modal method [29]. We then examine the predictive power of the retrieved admittance by calculating the coefficients r_- and t_- upon illumination in the backward direction. We also do the same procedure to predict r_+ and t_+ using the admittance retrieved from r_- and t_-. If both retrieved admittances from two illumination directions were practically equal to each other and the predictions for $r_{\pm}$ and $t_{\pm}$ were equal to their direct calculations, our homogenization model that considers only an admittance is recognized to be sufficient. Otherwise, we need to introduce the more sophisticated model that considers the bianisotropy ($Z_{\pm} \neq 0$) and have to retrieve additionally two nonidentical impedances Z_+ and Z_- using the full set of Eqs. (4).

In the following, we consider three examples: first, the motivating example of a nanostructured layer of graphene on top of a substrate; second, a very thin metasurface made from gold nanopatches (these examples are grouped in Sec. III A); third, a thick metasurface made from gold nanopatches. This example is studied in Sec. III B. We will see that the first two examples do not require a bianisotropy to effectively describe the metasurface whereas the third does. The transition from a thin to a thick metasurface is studied afterwards in more detail.

A. Very thin metasurfaces

As we mentioned earlier in the Introduction, for an array of graphene particles on top of a substrate we could not observe a bianisotropic response using our old homogenization model of Ref. [10], which was only suitable for a specific illumination direction. Here, we perform a homogenization with the tool presented in this paper and inspect if the bianisotropy is required to characterize a substrated nanostructured graphene layer.

We consider a periodic square array of graphene nanopatches located on top of a substrate with relative permittivity $\varepsilon_r = 10$. The permittivity of the substrate has been chosen generically realistic to some extent but sufficiently large in anticipation of a strong possible SIB effect [10]. In this example, the width of each nanopatch is $W = 1$ μm while the array period is $a = 2$ μm. A chemical potential of $\mu_c = 500$ meV is applied to graphene having the intrinsic loss factor [30] $\Gamma = 1$ meV. Such graphene patches experience a plasmon resonance in the far-infrared range [31–33].

The thickness of a monolayer graphene is as small as that of a single atom. Graphene is, therefore, characterized by a complex surface conductivity. However, in order to calculate for the reflection and transmission of an array of graphene patches, it can be adequately modeled as an array of patches of an effective medium with 1 nm thickness [30]. In our numerical simulations, we use this model of graphene [30]. We expected that this metasurface can be characterized by only an admittance parameter Y. Therefore, in accordance with our insight, the SIB should not arise. With this assumption, Eqs. (3) and (4) reduce to

$$r_{\mp} = \frac{\mp A_- - Y}{A_+ + Y}, \tag{10a}$$

$$t = \frac{2}{A_+ + Y}, \tag{10b}$$

$$Y_{\pm} = \frac{\pm A_- - A_+ r_{\pm}}{(1 + r_{\pm})}, \tag{10c}$$

where $A_{\pm}$ is given in Eq. (6b). Since the admittance Y is independent of the illumination direction, both equations in Eq. (10c) must provide practically the same results if this simple model is correct. The retrieved parameter Y versus frequency for both illumination directions is plotted in Fig. 3(a). Forward illumination corresponds to dashed lines, and the backward one to solid lines. One can see that the simple model works here. First, both values are practically identical in the entire frequency range. Second, the dispersion of the retrieved Y satisfies the passivity and causality constraints (see, e.g., in Ref. [34]).

Next, we predict the reflectance and transmittance for forward/backward illumination with the admittance retrieved from data corresponding to the backward/forward illumination [see Figs. 3(b) and 3(c)]. As it is clear from this figure, the retrieved admittance perfectly predicts reflectance and transmittance $|r|$ and $|t|$. Also, we see on Figs. 3(b) and 3(c) that the reflectance is asymmetric $\{|r_+| \neq |r_-|\}\rfloor_{f_r}$, where f_r is the resonance frequency band of the sheet admittance. We observe a resonant maximum for the forward illumination in the same range as a resonant minimum for the backward one.

This resonant asymmetry can be explained without the need of bianisotropy as follows. At the plasmon resonance, the sheet impedance $1/Y$ of the metasurface is a real value R. The wave incident from the substrate has low impedance η_- due to high ε_-. The value R is in-between this low impedance and that of free space, i.e., the metasurface operates as a matching device. This matching is frequency selective due to resonant dispersion of Y. The input impedance of the metasurface is a parallel connection of $1/Y$ and impedance of free space η_+. Within the resonance band there is a frequency at which the matching condition $1/\eta_- \approx 1/\eta_+ + 1/Y$ is satisfied with minimal error. However, when the wave is incident from free space it has high impedance η_+, and the same metasurface produces the resonant mismatch. In this case, the input impedance of the interface is the parallel connection of $1/Y$ and the low impedance η_-. In this case, we observe the resonant mismatch. The resonance of Y is so that the resonant value of $1/Y$ is in-between η_- and η_-. This results in the resonant maximum for the forward reflectance and the

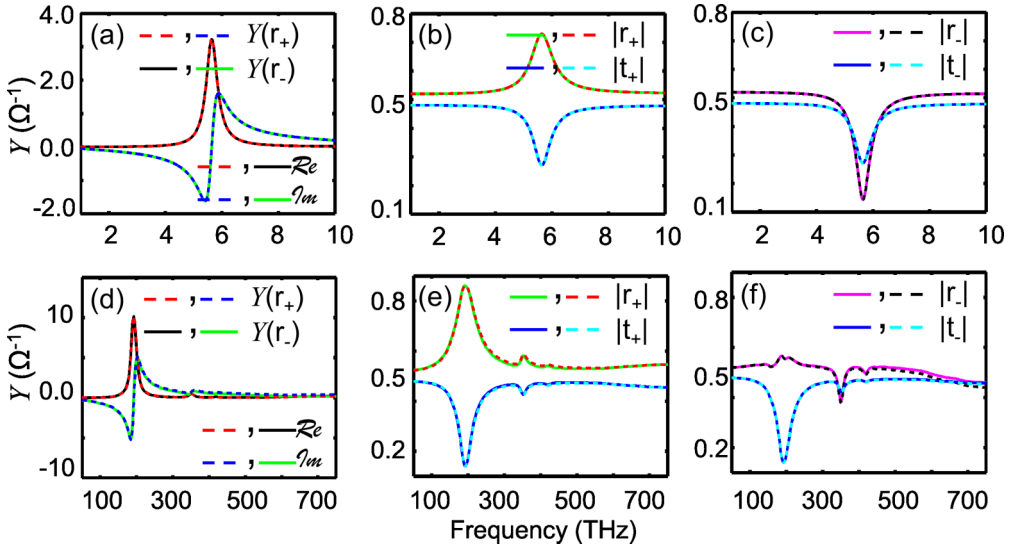

FIG. 3. (Color online) (a) Effective admittance Y retrieved from reflection coefficient r_+ (dashed lines) and r_- (solid lines) for graphene nanopatches; real (red and black lines) and imaginary (blue and green lines) parts. (b) The forward reflectance $|r_+|$ (solid green line) and the transmittance $|t_+|$ (solid blue line) predicted via $Y(r_-)$ retrieved from the data for backward illumination compared with the rigorous reflectance (dashed red line) and transmittance (dashed cyan line) calculated using full wave simulations. (c) The backward reflectance $|r_-|$ (solid magenta line) and the transmittance $|t_-|$ (solid blue line) predicted via $Y(r_+)$ retrieved from the data for forward illumination compared with the rigorous reflectance (dashed black line) and transmittance (dashed cyan line) calculated using full wave simulations. (d), (e), (f) Corresponding plots similar to (a), (b), and (c) for gold nanopatches of thickness $d = 5$ nm.

resonant minimum for the backward reflectance. It is so only for graphene nanopatches. For gold nanopatches, as considered further below, such observation does not withstand a detailed analysis since the resonant value of $1/Y$ is much larger.

Since the thickness of a graphene sheet is as thin as a single atomic layer, we hypothesized that potentially the reason for the absence of bianisotropy in the effective description is related to the thickness. We consequently examine the thickness effect on the bianisotropy response of an array of gold nanopatches.

We considered at first a periodic square array of gold (material parameters of gold are taken from Ref. [35]) nanopatches located on a substrate with relative permittivity $\varepsilon_r = 10$. The lateral dimension of each patch is $W = 100$ nm while the array period is $a = 200$ nm. Each nanopatch has a thickness of $d = 5$ nm. This is much smaller than the skin depth δ of gold. In the frequency range of interest, i.e., 200–300 THz, δ varies from 24 to 55 nm. Such a thin metasurface should be also characterized through only an effective shunt admittance if our hypothesis is correct, and it is really so. Figures 3(d)–3(f) represent similar plots for gold nanopatches as Figs. 3(a)–3(c) for graphene nanopatches. Again, admittances are identical when compared for forward and backward illumination directions and properties retrieved for a specific illumination direction can be used to predict the optical response for the opposite illumination direction. Indeed, the internal electric field should be symmetrically distributed across such a thin patch.

Now, in order to study this surprising result and to link it to previous findings that suggested the requirement of an effective bianisotropy to describe metasurfaces made from plasmodic inclusions on top of a substrate, we continue to study thick gold nanopatches.

B. Substantially thick metasurfaces

We consider a planar array of gold nanopatches similar to the previous example, but we increase the patch thickness d so that it exceeds the skin depth in the frequency range of interest. To be specific, we have been chosing $d = 40$ nm and performed the same procedure as before. First, we retrieve the effective admittance Y from the forward/backward illumination, using Eq. (10c), i.e., assuming that the SIB is negligible. In Fig. 4(a), the forward incidence corresponds to dashed lines, and the backward one to solid lines.

Second, we use the retrieved value in order to predict the reflectance and transmittance for the opposite illumination and compare these predictions to full wave simulations for the same situation. Besides the different admittance when retrieved for a forward and a backward illumination, we see from Figs. 4(b) and 4(c) that both predicted (solid lines) reflectance and transmittance for an illumination from the opposite side deviate notably from the simulated curves (dashed lines). Therefore, this metasurface cannot be characterized only by a shunt admittance, and we have to take into account the SIB.

The retrieved admittance and impedances using the complete model based on Eqs. (4) are plotted in Figs. 5(a) and 5(b). These retrieved parameters satisfy the passivity and causality constraints and properly predict the electromagnetic behavior of the substrated metasurface. The predicted values of the reflectance and transmittance and the results from full wave simulations are plotted in Fig. 5(c). A perfect agreement (visual coincidence of dashed and solid lines) is seen in this figure. Figure 6 illustrates the effect of SIB and explains its absence in the case of thin nanopatches. In Figs. 6(a) and 6(b), the absolute value of the normalized electric field for an illumination in forward direction in the central cross section of the unit cell are shown for two cases: $d = 5$ and 40 nm, respectively. The

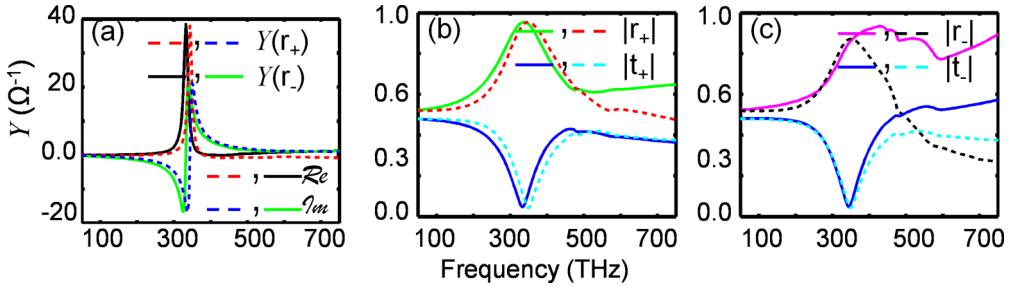

FIG. 4. (Color online) (a) Effective admittance Y retrieved from reflection coefficient r_+ (dashed lines) and r_- (solid lines) for a periodic array of gold nanopatches of thickness $d = 40$ nm; real (red and black lines) and imaginary (blue and green lines) parts. (b) The forward reflectance $|r_+|$ (solid green line) and transmittance $|t_+|$ (solid blue line) predicted via $Y(r_-)$ retrieved from the data for backward illumination compared with the rigorous reflectance (dashed red line) and transmittance (dashed cyan line) calculated using full wave simulations. (c) The backward reflectance $|r_-|$ (solid magenta line) and transmittance $|t_-|$ (solid blue line) predicted via $Y(r_+)$ retrieved from the data for forward illumination compared with the rigorous reflectance (dashed black line) and transmittance (dashed cyan line) calculated using full wave simulations.

fields are plotted at 193 THz for the thin and at 345 THz for the thick metasurface, respectively. However, similar features occur at all frequencies in the range of the plasmon resonance. In the case of the thin metasurface, the spatial variation of the electric field across the nanopatch is only ±20% with respect to the mean value of the electric field amplitude. In contrast, for the thick metasurface the corresponding field variations are sevenfold. Here, small hot spots are formed at the edges of the patches with the evident parity of the field localization in two different spatial domains: that inside the nanopatch and that inside the substrate. Indeed, the combined field localization in the epsilon-negative material of the patch and the epsilon-positive material of the substrate offer the resonant magnetic mode. This magnetic mode is induced by the electric field, i.e., the bianisotropy of the electromagnetic response (see in Ref. [14]). The strong asymmetry in the field localization with respect to the nanopatch, i.e., the hot spot, is the consequence of the interference between the dipole induced in the nanopatch and the mirror dipole in the substrate. In case of the thin metasurface, the patch is fully penetrable for the external field and the field localization is symmetric with respect to the nanopatch. Although a finite portion is also located in the substrate, the field averaged over this portion (and therefore its polarization) remains much smaller than that inside the patch. Therefore, no magnetic mode is induced in the metasurface. We do not encounter the necessity to consider bianisotropy in the effective description of such a thin metasurface.

To better illustrate the link between physical thickness of patches and the SIB effect, a parametric study would be useful. In the next section, we perform such study, which is based on calculations of error functions.

IV. PARAMETRIC STUDY: METASURFACE THICKNESS AND SIB

In this section, we use the same array of gold nanopatches without changing their widths and the array period. However, we study the effect of variation of metasurface thickness on the predicted reflectance and transmittance. We use the simple admittance model Y in Eq. (10) to predict the reflectance/transmittance in order to calculate the error level associated with the proposed model for the description of substrated metasurfaces. We define the following error functions:

$$\zeta_{r_\pm}(f) = \left| \frac{|r_\pm^{\mathrm{pred}}(f)| - |r_\pm^{\mathrm{calc}}(f)|}{|r_\pm^{\mathrm{calc}}(f)|} \right|, \tag{11a}$$

$$\zeta_{t_\pm}(f) = \left| \frac{|t_\pm^{\mathrm{pred}}(f)| - |t_\pm^{\mathrm{calc}}(f)|}{|t_\pm^{\mathrm{calc}}(f)|} \right|, \tag{11b}$$

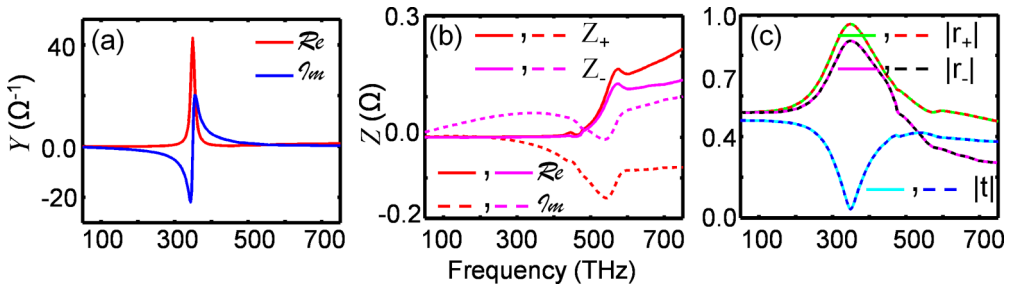

FIG. 5. (Color online) (a) Effective admittance Y retrieved using Eq. (4b) for a periodic array of gold nanopatches of thickness $d = 40$ nm. (b) Effective impedances Z_+ and Z_- retrieved using Eq. (4a) for the same array. (c) Both the forward and backward reflectances $|r_+|$ and $|r_-|$ and transmittance $|t|$ predicted using Eq. (3) from retrieved impedances Z_+ and Z_- and admittance Y compared with the reflectance and transmittance calculated using full wave simulations. Dashed lines correspond to the simulated results and solid lines to the predicted results.

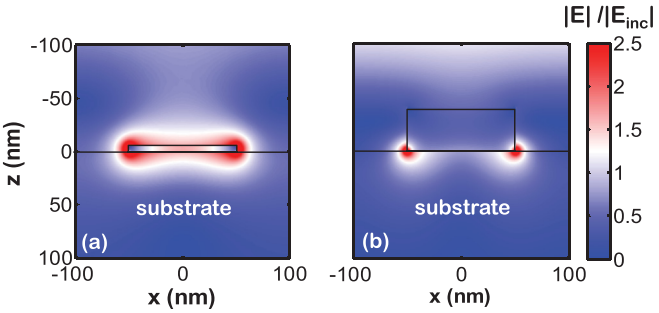

FIG. 6. (Color online) Amplitude of the normalized electric field in the central vertical cross section of the unit cell for two metasurfaces of gold nanopatches. (a) Symmetric distribution in the case $d = 5$ nm. (b) Asymmetric distribution for $d = 40$ nm. The SIB effect corresponds to this case.

that depend here on frequency. $|r_{\pm}^{\text{pred}}(f)|$, $|t_{\pm}^{\text{pred}}(f)|$, $|r_{\pm}^{\text{calc}}(f)|$, and $|t_{\pm}^{\text{calc}}(f)|$ are the predicted and numerically calculated reflectance/transmittance, respectively. "+" sign refers to the case when we use the backward reflection data to predict forward reflectance and transmittance $|r_+|$ and $|t_+|$ while "−" refers to the opposite case when we use the forward reflection data to predict backward reflectance and transmittance $|r_-|$ and $|r_-|$. For this purpose, Eqs. (10) are used. Figures 7(a) and 7(b) show these errors for two cases: one of them is the case when the metasurface thickness is much smaller than the skin depth in the desired frequency range, i.e., $d = 5$ nm (solid lines) and the other when it is in the order of skin depth, i.e., $d = 25$ nm (dashed lines). As it is clear from these plots, the maximum error for the thin metasurface ($d = 5$ nm) is only ∼4%. This maximum error occurs ar high frequencies in the forward reflectance $|r_+|$ [Fig. 7(b)] while an error of ∼100% is associated with the backward reflectance and forward transmittance of thicker metasurface. Notice the minimum error is associated with $|t_-|$ at low frequencies and it is 0.003% and 0.1% for $d = 5$ and 25 nm, respectively.

To be able to quantify the deviations more systematically, we introduce a cumulative error. This allows for clarifying the threshold where the thickness effect starts to be significant for the homogenization modeling. We define the cumulative error functions

$$\zeta_{cr_{\pm}} = \left| \frac{\sqrt{\int_f \left[|r_{\pm}^{\text{pred}}(f)| - |r_{\pm}^{\text{calc}}(f)|\right]^2 df}}{\int_f |r_{\pm}^{\text{calc}}(f)| df} \right|, \quad (12a)$$

$$\zeta_{ct_{\pm}} = \left| \frac{\sqrt{\int_f \left[|t_{\pm}^{\text{pred}}(f)| - |t_{\pm}^{\text{calc}}(f)|\right]^2 df}}{\int_f |t_{\pm}^{\text{calc}}(f)| df} \right|, \quad (12b)$$

which are integrations over the whole frequency band under consideration. Then, we find these cumulative errors for a thickness range of $(1 < d < 50)$ nm. These errors are plotted in Fig. 7(c) for the frequency range of $(50 < f < 600)$ THz, which covers our resonance band for all examples. Note that the resonance frequency for $d = 1$ nm is ∼90 THz while it is ∼355 THz for $d = 50$ nm. It is clear from Fig. 7(c) that the maximum cumulative error is less than 40% for $d = 50$ nm and appeared in $|r_-|$ when we have used the data of reflection from forward illumination to retrieve admittance Y. The minimum is ∼0.007% for $d = 1$ nm and appeared in $|t_-|$. It can be also seen from this figure that for $d \leqslant 14$ nm, which is roughly one half of skin depth δ of gold at this frequency band, the maximum cumulative error is less than 5%. This error level shall be defined here as the maximum admissible level for the cumulative error. The thickness associated with this error level is the threshold from which we suggest to consider the more sophisticated circuit model for representation of the substrated metasurface. Indeed, when $d > \delta$, the electric field inside the nanopatch is not anymore uniform due to the skin effect. Therefore, in accordance to Ref. [14], a hot spot arises at the boundary between metal particles and substrate evolving a magnetoelectric (bianisotropy) response. Electric dipoles of metal particles and those of hot spots located in the substrate form an effective magnetic sheet. For the forward incidence, the reflected field is produced by the surface electric polarization, surface magnetic polarization, and bulk electric polarization of the substrate according to the transmitted plane wave. In the case of thin nanopatches, the electric field is spread uniformly in the nanopatch even at the plasmon resonance and the local field enhancement in the substrate beneath the particle does not arise. Then, the magnetoelectric response referred to the interface is negligible, and the reflected field is practically a sum of that produced by an electric surface polarization

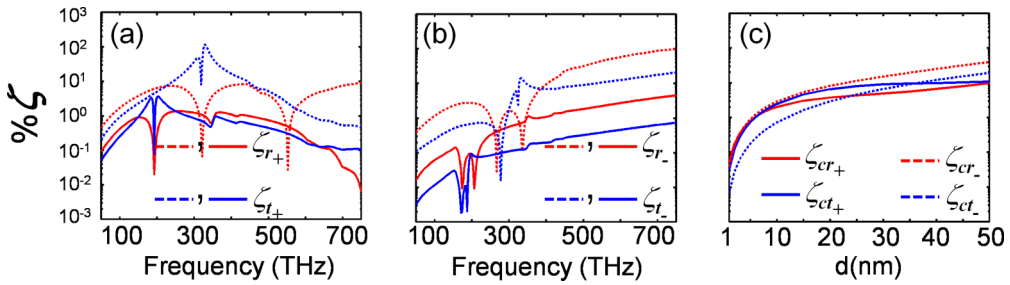

FIG. 7. (Color online) (a) Forward direction error analysis [see Eq. (11)] for predicted reflectance $|r_+|$ (red lines) and transmittance $|t_+|$ (blue lines) as a function of frequency for two substrated metasurfaces with two different thicknesses: $d = 5$ nm (solid lines) and $d = 25$ nm (dashed lines). (b) The same plots as in the previous case but for the prediction of backward parameters. (c) Cumulative error analysis [see Eq. (12)] versus metasurface thickness for the frequency band of $(50 < f < 600)$ THz. Notice, the vertical axis is in logarithmic scale.

and bulk electric polarization of the substrate. Eventually, we would like to stress that an absolute value in the error from which it is required to resort for an effective description to the more advanced model that takes the bianisotropy in account cannot be given. Here, for each specific purpose such threshold has to be identified.

V. CONCLUSIONS

We may summarize our achievements in this study as follows:

(i) If a resonant metasurface is located on top of a highly refractive substrate, its reflectance asymmetry upon illumination from two different directions and its bianisotropy are two effects that can independently appear; the bianisotropy can not only increase but also decrease (and even fully suppress) the reflectance asymmetry.

(ii) The reflectance asymmetry of a nonbianisotropic substrated metasurface arises due to the optical contrast between the two surrounding media and the presence of losses. Moreover, a resonance in the losses only causes this asymmetry to be resonant as well.

(iii) An electrically resonant metasurface on top of a highly refractive substrate does not necessarily imply a bianisotropy, e.g., a metasurface of plasmonic patches thinner than the skin depth can be described as a sheet of electric surface current only.

(iv) A metasurface composed of flat plasmonic patches, which are thicker than the skin depth of the metal, located on a highly refractive substrate, contain both electric and magnetic polarization responses. The last one refers to substrate-induced bianisotropy.

In our retrieval procedure, we have used the circuit model of the metasurface, however, we also inspected the distributions of electromagnetic fields and checked that they correspond to our physical insight. To quantitatively describe the SIB effect we have performed a parametric study of the error related with neglected bianisotropy. Our work is both an original research and educationally valuable study, which seems to be important in view of rapid development of metasurfaces nowadays.

ACKNOWLEDGMENTS

This work was supported by the Deutsche Forschungsgemeinschaft within Project No. RO 3640/3-1. The authors are grateful to S. Tretyakov for useful discussions.

APPENDIX: RELATION BETWEEN CIRCUIT PARAMETERS AND EFFECTIVE MATERIAL PARAMETERS

Here, we briefly present the way to extract the relation between the effective material parameters and the circuit parameters for an omega-type metasurface. The methodology for a general bianisotropic metasurface may be published in a separate work. This is done with the purpose to provide an unambiguous link between the language of circuit parameters as potentially used by a more engineering oriented community and those of polarizabilities as potentially used by a more physics-oriented community.

Let us first consider the same metasurface as in Sec. II and Fig. 2. Moreover, we maintain the same constraints and limitations such as normal illumination, optically dense planar array, etc. With those limitations, recalling from Refs. [10,14,25], the constitutive relations between the induced surface polarizations P_x and M_y and the average fields E_x^{ave} and H_y^{ave} for the proposed omega-type metasurface at normal incidence may read as

$$P_x = \hat{\chi}_{xx}^{\mathrm{ee}} E_x^{\mathrm{ave}} + \hat{\chi}_{xy}^{\mathrm{em}} H_y^{\mathrm{ave}}, \tag{A1a}$$

$$M_y = \hat{\chi}_{yx}^{\mathrm{me}} E_x^{\mathrm{ave}} + \hat{\chi}_{yy}^{\mathrm{mm}} H_y^{\mathrm{ave}}. \tag{A1b}$$

In Eqs. (A1a) and (A1b), parameters $\hat{\chi}_{xx}^{\mathrm{ee}}$, $\hat{\chi}_{xy}^{\mathrm{em}}$, $\hat{\chi}_{yx}^{\mathrm{me}}$, and $\hat{\chi}_{yy}^{\mathrm{mm}}$ are effective electric, magnetoelectric, electromagnetic, and magnetic surface susceptibilities, respectively. Moreover, the average fields are denoted by

$$E_x^{\mathrm{ave}} = \frac{E_+ + E_-}{2}, \tag{A2a}$$

$$H_x^{\mathrm{ave}} = \frac{H_+ + H_-}{2}, \tag{A2b}$$

where $E_\pm$ and $H_\pm$ are the total fields taken at the metasurface plane (here at $z = 0$) and depend on the illumination direction. These fields can have the superscript F or B depending on whether the forward or backward illumination is considered. For the forward illumination direction, these total fields are denoted by

$$E_+^{\mathrm{F}} = E_x^{\mathrm{i}} + E_x^{\mathrm{r}}, \qquad E_-^{\mathrm{F}} = E_x^{\mathrm{t}}, \tag{A3a}$$

$$H_+^{\mathrm{F}} = H_x^{\mathrm{i}} + H_x^{\mathrm{r}}, \qquad H_-^{\mathrm{F}} = H_x^{\mathrm{t}},, \tag{A3b}$$

and for the backward illumination direction they are denoted by

$$E_+^{\mathrm{B}} = E_x^{\mathrm{t}}, \qquad E_-^{\mathrm{B}} = E_x^{\mathrm{i}} + E_x^{\mathrm{r}}, \tag{A4a}$$

$$H_+^{\mathrm{B}} = H_x^{\mathrm{t}}, \qquad H_-^{\mathrm{B}} = H_x^{\mathrm{i}} + H_x^{\mathrm{r}}. \tag{A4b}$$

In Eqs. (A3a)–(A4b), the superscripts i, r, and t correspond to the incident, reflected, and transmitted fields, respectively, taken at the metasurface plane. Now, we may take advantage of Maxwell's boundary conditions for the tangential electric and magnetic fields $E_\pm$ and $H_\pm$ derived in Refs. [10,14,25], i.e.,

$$E_+^F - E_-^F = -i\omega M_y, \tag{A5a}$$

$$H_+^F - H_-^F = -i\omega P_x \tag{A5b}$$

for forward and

$$E_+^B - E_-^B = i\omega M_y, \tag{A6a}$$

$$H_+^B - H_-^B = -i\omega P_x \tag{A6b}$$

for backward illumination directions, respectively. Now, applying (A1a)–(A4b) into (A5a)–(A6b) and considering $\hat{\chi}_{xy}^{\mathrm{em}} = -\hat{\chi}_{yx}^{\mathrm{me}}$ for an omega-type bianisotropy [11], we obtain the following two relations between total fields for the forward:

$$E_+^{\mathrm{F}} = \frac{A_0 C_0 + (1 - B_0)^2}{2A_0} H_+^{\mathrm{F}} - \frac{-A_0 C_0 + (1 - B_0)^2}{2A_0} H_-^{\mathrm{F}}, \tag{A7a}$$

$$E_-^{\mathrm{F}} = \frac{-A_0C_0 + (1-B_0)^2}{2A_0} H_+^{\mathrm{F}} - \frac{A_0C_0 + (1+B_0)^2}{2A_0} H_-^{\mathrm{F}} \tag{A7b}$$

and backward

$$E_-^{\mathrm{B}} = \frac{A_0C_0 + (1+B_0)^2}{2A_0} H_+^{\mathrm{B}} - \frac{-A_0C_0 + (1-B_0)^2}{2A_0} H_-^{\mathrm{B}}, \tag{A8a}$$

$$E_+^{\mathrm{B}} = \frac{-A_0C_0 + (1-B_0)^2}{2A_0} H_+^{\mathrm{B}} - \frac{A_0C_0 + (1-B_0)^2}{2A_0} H_-^{\mathrm{B}} \tag{A8b}$$

illumination directions, respectively. In (A7a)–(A8b) we used the following abbreviations:

$$A_0 = -i\frac{\omega}{2}\hat{\chi}_{xx}^{\mathrm{ee}}, \quad B_0 = -i\frac{\omega}{2}\hat{\chi}_{xy}^{\mathrm{em}}, \quad C_0 = -i\frac{\omega}{2}\hat{\chi}_{yy}^{\mathrm{mm}}. \tag{A9}$$

On the other hand, we know that for a *T-circuit* model represented in Fig. 2(b), one may write the following sets of equations between the input and output voltages and currents through the circuit parameters for different illumination directions, respectively:

$$V_\pm^{\mathrm{i}} = \left(\frac{1}{Y} + Z_\pm\right) I_\pm^{\mathrm{i}} + \left(\frac{1}{Y}\right) I_\pm^{\mathrm{o}}, \tag{A10a}$$

$$V_\pm^{\mathrm{o}} = \left(\frac{1}{Y}\right) I_\pm^{\mathrm{i}} + \left(\frac{1}{Y} + Z_\mp\right) I_\pm^{\mathrm{o}}. \tag{A10b}$$

Comparing the last two equations with Eqs. (A7a)–(A8b), one may find the following relations between the circuit parameters Y and $Z_\pm$ and the effective material parameters $\hat{\chi}_{xx}^{\mathrm{ee}}$, $\hat{\chi}_{yy}^{\mathrm{mm}}$, and $\hat{\chi}_{xy}^{\mathrm{em}}$:

$$\frac{2}{Y} = \frac{A_0C_0 - (1-B)^2}{A_0}, \tag{A11a}$$

$$Z_+ = \frac{A_0C_0 - B(1-B)}{A_0}, \tag{A11b}$$

$$Z_- = \frac{A_0C_0 + B(1+B)}{A_0} \tag{A11c}$$

or, inversely,

$$A_0 = -i\frac{\omega}{2}\hat{\chi}_{xx}^{\mathrm{ee}} = \frac{2}{Z_+ + Z_- + \frac{4}{Y}}, \tag{A12a}$$

$$B_0 = -i\frac{\omega}{2}\hat{\chi}_{xy}^{\mathrm{em}} = \frac{Z_- - Z_+}{Z_+ + Z_- + \frac{4}{Y}}, \tag{A12b}$$

$$C_0 = -i\frac{\omega}{2}\hat{\chi}_{yy}^{\mathrm{mm}} = 2\frac{Z_-Z_+ + \frac{1}{Y}(Z_- + Z_+)}{Z_+ + Z_- + \frac{4}{Y}}. \tag{A12c}$$

It is obvious from these equations that for equality $Z_- = Z_+ = Z$, the effective magnetoelectric susceptibility $\hat{\chi}_{xy}^{\mathrm{em}}$ becomes zero, which implies no bianisotropy in the effective material parameter paradigm. Moreover, the effective magnetic susceptibility $\hat{\chi}_{yy}^{\mathrm{mm}}$ reduces to $2Z$, which is consistent with our assertions in the paper. Furthermore, if there is no magnetic response, i.e., $Z = \hat{\chi}_{yy}^{\mathrm{mm}} = 0$, then the effective electric susceptibility $\hat{\chi}_{xy}^{\mathrm{ee}}$ reduces to Y, which again implies a consistent circuit modeling for the proposed omega-type metasurface.

[1] J. B. Pendry, Phys. Rev. Lett. **85**, 3966 (2000).
[2] D. R. Smith, J. B. Pendry, and M. C. K. Wiltshire, Science **305**, 788 (2004).
[3] N. Engheta and R. Ziolkowski, *Metamaterials Physics and Engineering Explorations* (Wiley, New York, 2006).
[4] F. Capolino, *Applications of Metamaterials* (CRC Press, New York, 2009).
[5] A. K. Sarychev and V. A. Shalaev, *Electrodynamics of Metamaterials* (World Scientific, Singapore, 2007).
[6] Y. Feng, J. Zhao, X. Teng, Y. Chen, and T. Jiang, Phys. Rev. B **75**, 155107 (2007).
[7] J. Yao, Z. Liu, Y. Liu, Y. Wang, C. Sun, G. Bartal, A. M. Stacy, and X. Zhang, Science **321**, 930 (2008).
[8] X. Huang, Y. Zhang, S. T. Chui, and L. Zhou, Phys. Rev. B **77**, 235105 (2008).
[9] H. O. Moser and Carsten Rockstuhl, Laser Photon. Rev. **6**, 219 (2012).
[10] M. Albooyeh and C. R. Simovski, J. Opt. **13**, 105102 (2011).
[11] A. Serdyukov, I. Semchenko, S. Tretyakov, and A. Sihvola, *Electromagnetics of Bi-anisotropic Materials: Theory and Applications* (Gordon and Breach, Amsterdam, 2001).
[12] D. Powell and Y. S. Kivshar, Appl. Phys. Lett. **97**, 091106 (2010).
[13] L. Novotny, Phys. Rev. Lett. **98**, 266802 (2007).
[14] M. Albooyeh, D. Morits, and C. Simovski, Metamaterials **5**, 178 (2011).
[15] Omega particles are constitutive elements of microwave bianisotropic metamaterials [3–5].
[16] A. Minovich, D. N. Neshev, D. Powell, and Y. S. Kivshar, Opt. Commun. **283**, 4770 (2010).
[17] C. Saeidi and D. van der Weide, Appl. Phys. Lett. **103**, 183101 (2013).
[18] S. Yun, Z. H. Jiang, Q. Xu, Z. Liu, D. H. Werner, and T. S. Mayer, ACS Nano **6**, 4475 (2012).
[19] Z. H. Jiang, S. Yun, L. Lin, J. A. Bossard, D. H. Werner, and T. S. Mayer, Sci. Rep. **3**, 01571 (2013).
[20] Z. H. Jiang and D. H. Werner, Opt. Express **21**, 5594 (2013).
[21] By reflectance we mean the amplitude of the reflection coeffiecient.
[22] Y. Ra'di, V. S. Asadchy, and S. A. Tretyakov, IEEE Trans. Antennas Propag. **61**, 4606 (2013).
[23] R. Alaee, M. Albooyeh, M. Yazdi, N. Komjani, C. R. Simovski, F. Lederer, and C. Rockstuhl, Phys. Rev. B **91**, 115119 (2015).
[24] M. Albooyeh and C. Simovski, Opt. Express **20**, 21888 (2012).

[25] C. L. Holloway, E. F. Kuester, J. A. Gordon, J. O'Hara, J. Booth, and D. R. Smith, IEEE Antennas Propag. Mag. **54**, 10 (2012).
[26] M. Albooyeh, Y. Ra'di, M. Q. Adil, and C. R. Simovski, Phys. Rev. B **88**, 085435 (2013).
[27] R. Alaee, C. Menzel, U. Huebner, E. P. Severin, S. B. Hasan, T. Pertsch, C. Rockstuhl, and F. Lederer, Nano Lett. **13**, 3482 (2013).
[28] D. M. Pozar, *Microwave Engineering* (Wiley, Hoboken, NJ, 2009).
[29] L. Li, J. Opt. Soc. Am. A **14**, 2758 (1997).
[30] R. Alaee, M. Farhat, C. Rockstuhl, and F. Lederer, Opt. Express **20**, 28017 (2012).
[31] A. Y. Nikitin, F. Guinea, F. J. Garcia-Vidal, and L. Martin-Moreno, Phys. Rev. B **85**, 081405 (2012).
[32] F. H. Koppens, D. E. Chang, and F. J. Garcia de Abajo, Nano Lett. **11**, 3370 (2011).
[33] J. Chen, M. L. Nesterov, A. Y. Nikitin, S. Thongrattanasiri, P. Alonso-González, T. M. Slipchenko, F. Speck, M. Ostler, T. Seyller, I. Crassee, F. H. Koppens, L. Martin-Moreno, F. J. García de Abajo, A. B. Kuzmenko, and R. Hillenbrand, Nano Lett. **13**, 6210 (2013).
[34] A. Alù, Phys. Rev. B **83**, 081102(R) (2011).
[35] P. B. Johnson and R. W. Christy, Phys. Rev. B **6**, 4370 (1972).